

# Genetic Analysis of a Metazoan Pathway using Transcriptomic Phenotypes, Supplementary Information

David Angeles-Albores<sup>1, 2,†</sup> Carmie Puckett Robinson<sup>1, 2, 3,†</sup> Brian A. Williams<sup>1</sup>  
Barbara J. Wold<sup>1</sup> Paul W. Sternberg<sup>1, 2, \*</sup>

June 12, 2017

† These authors contributed equally to this work

**1** Division of Biology and Biological Engineering, Caltech, Pasadena, CA, 91125, USA

**2** Howard Hughes Medical Institute, Caltech, Pasadena, CA, 91125, USA

**3** Department of Neurology, Keck School of Medicine, University of Southern California, Los Angeles, California, 90033, USA

\* Corresponding author. Contact: pws@caltech.edu

## A quality check of the transcriptomic data reveals excellent agreement with the literature

One way to establish whether genes are acting additively or epistatically to each other is to perform qPCR of a reporter gene in the single and double mutants. This approach was used to successfully map the relationships within the hypoxia pathway (see, for example<sup>1,2</sup>). A commonly used hypoxia reporter gene is *nhr-57*, which is known to exhibit a several-fold increase in mRNA expression when HIF-1 accumulates<sup>2,3,4</sup>. Likewise, increased HIF-1 function is known to cause increased transcription of *rhy-1* and *egl-9*<sup>5</sup>.

We can selectively look at the expression of a few genes at a time. Therefore, we queried the changes in expression of *rhy-1*, *egl-9*, and *nhr-57*. We included the nuclear laminin gene *lam-3* as a representative negative control not believed to be responsive to alterations in the hypoxia pathway. *nhr-57* was upregulated in *egl-9(lf)*, *rhy-1(lf)* and *vhl-1(lf)*, but remains unchanged in *hif-1(lf)*. *egl-9(lf);vhl-1(lf)* had an expression level similar to *egl-9(lf)*; whereas the *egl-9(lf) hif-1(lf)* mutant showed wild-type levels of the reporter expression, as reported previously<sup>2</sup> (see Fig. S1).

We observed changes in *rhy-1(lf)* expression consistent with previous literature<sup>2</sup> when HIF-1 accumulates. We also observed increases in *egl-9* expression in *egl-9(lf)*. *egl-9* is known as a hypoxia responsive gene<sup>5</sup>. Although changes in *egl-9* expression were not statistically significantly different from the wild-type in *rhy-1(lf)* and *vhl-1(lf)* mutants, the mRNA levels of *egl-9* still trended towards increased expression in these genotypes. As with *nhr-57*, *egl-9* and *rhy-1* expression were wild-type in *egl-9(lf) hif-1(lf)* and *egl-9(lf);vhl-1(lf)* mutant showed expression phenotypes identical to *egl-9(lf)*. This dataset also showed that knockout of *hif-1* resulted in a modest increase in the levels of *rhy-1*. This suggests that *hif-1*, in addition to being a positive regulator of *rhy-1* when strongly expressed, also inhibits *rhy-1*, which constitutes a novel observation. Using a single reporter we would have been able to reconstruct an important fraction of the genetic relationships between the genes in the hypoxia pathway—but would likely fail to observe yet other genetic interactions, such as the evidence for *hif-1* negatively regulating *rhy-1* transcript levels.

## Weighted Correlations

After we calculated the pairwise correlation within each STP, we weighted the result of each regression by the number of isoforms within the STP and divided by the total number of differentially expressed isoforms present in the two mutant transcriptomes that contributed to that specific STP,  $N_{\text{overlap}}/N_{g_1 \cup g_2}$ . The weighted regressions recapitulated a module network (see Fig. S3). We identified a strong positive

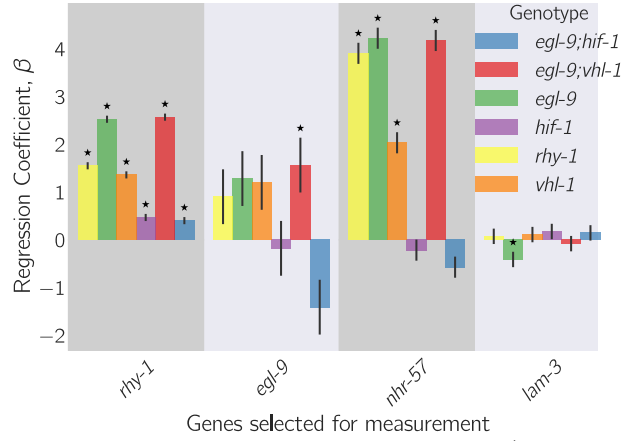


**Figure S1.** Observed  $\beta$  values of select genes. We selected four genes (*rhy-1*, *egl-9*, *nhr-57* and *lam-3*, shown on the x-axis) and plotted their regression coefficients,  $\beta$ , as measured for every genotype (represented by one of six colors) to study the epistatic relationships between each gene. Asterisks above a bar represent a regression coefficient statistically significantly different from 0 ( $q < 10^{-1}$ ) relative to a wild-type control. Error bars show standard error of the mean value of  $\beta$ . *nhr-57* is an expression reporter that has been used previously to identify *hif-1* regulators<sup>2,1</sup>. *lam-3* is shown here as a negative control that should not be altered by mutations in this pathway. We measured modest increases in the levels of *rhy-1* mRNA when *hif-1(lf)* is knocked out.

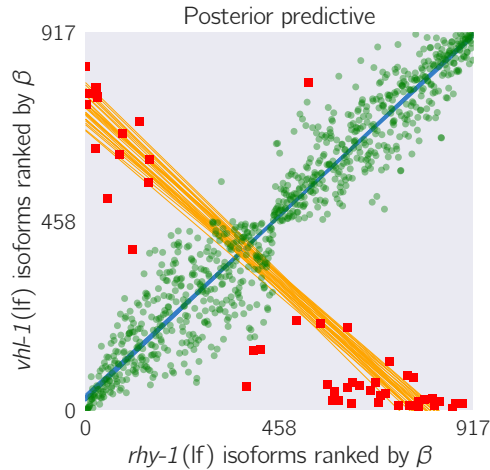


**Figure S2.** A feedback loop can generate transcriptomes that are both correlated and anti-correlated. The *vhl-1(lf)/rhy-1(lf)* STP shows a cross-pattern. Green large points are inliers to the first regression. Red squares are outliers to the first regression. Only the red small points were used for the secondary regression. Blue lines are representative samples of the primary bootstrapped regression lines. Orange lines are representative samples of the secondary bootstrapped regression lines.

interaction between *egl-9(lf)* and *rhy-1(lf)*. The magnitude of this weighted correlation derives from the number of genes that are differentially expressed for these mutants (2,549 and 3,005 DEGs respectively) and the size of their STP, which makes the weighting factor considerably larger than other pairs. The weak correlation between *hif-1(lf)* and *egl-9(lf)* results from the large effect size of the *egl-9(lf)* transcriptome coupled with the small STP between both mutants.

The fine-grained nature of transcriptional phenotypes means that these weighted correlations between transcriptomes of single mutants are predictive of genetic interaction.

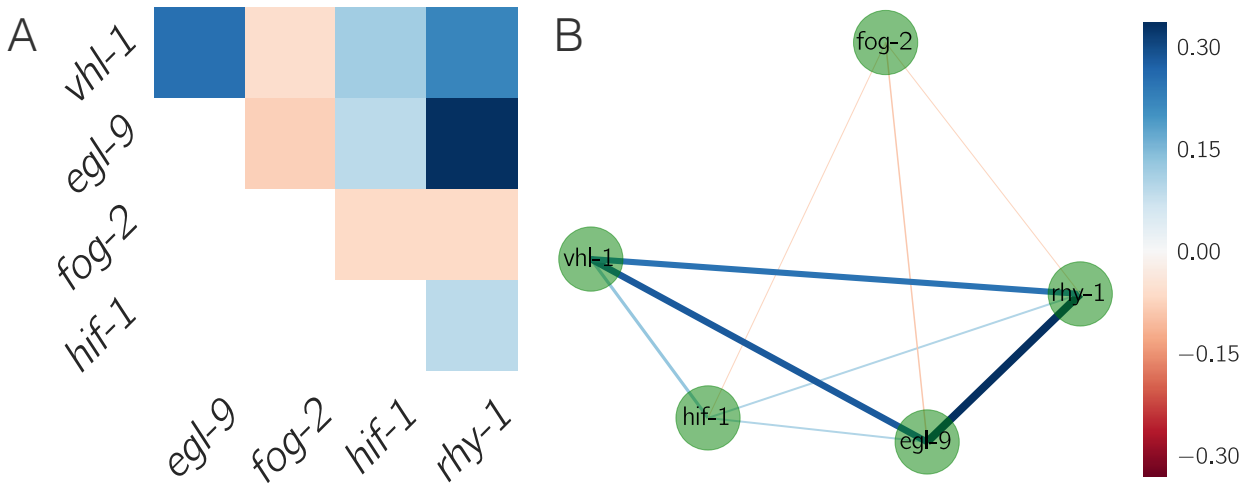


**Figure S3.** A. Heatmap showing pairwise regression values between all single mutants. B. Correlation network drawn from A. Edge width is proportional to the logarithm of the magnitude of the weighted correlation between two nodes divided by absolute value of the weighted correlation value of smallest magnitude. Edges are also colored according to the heatmap in A. Inhibitors of *hif-1* are tightly correlated and form a control module; *hif-1* is positively correlated to its inhibitors, albeit weakly; and *fog-2*, a gene that is not reported to interact with the hypoxia pathway, has the smallest, negative correlation to any gene.

### Enrichment analysis of the hypoxia response

To validate that our transcriptomes were correct, and to understand how biological functions may vary between them, we subjected each decoupled response to enrichment analysis using the WormBase Enrichment Suite<sup>67</sup>.

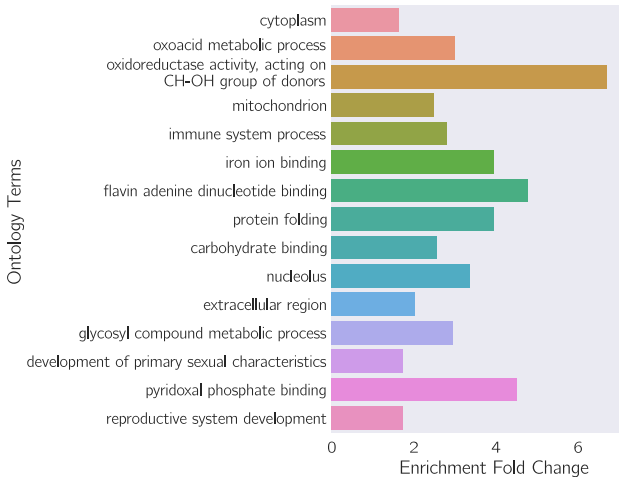


**Figure S4.** Gene ontology enrichment analysis of genes associated with the main hypoxia response. A number of terms reflecting catabolism and bioenergetics are enriched.

We used gene ontology enrichment analysis (GEA) on the main hypoxia response program. This showed that the terms ‘oxoacid metabolic process’ ( $q < 10^{-4}$ , 3.0 fold-enrichment, 24 genes), ‘iron ion binding’ ( $q < 10^{-2}$ , 3.8 fold-enrichment, 10 genes), and ‘immune system process’ ( $q < 10^{-3}$ , 2.9 fold-enrichment, 20 genes) were significantly enriched. GEA also showed enrichment of the term ‘mitochondrion’ ( $q < 10^{-3}$ , 2.5 fold-enrichment, 29 genes) (see Fig. S4). Indeed, *hif-1(lf)* has been implicated in all of these biological and molecular functions<sup>7,8,9,10</sup>. As benchmark on the quality of our data, we selected a set of 22 genes known to be responsive to HIF-1 levels from the literature and asked whether these genes were present in our hypoxia response list. We found 8/22 known genes, which constitutes a statistically significant result ( $p < 10^{10}$ ). The small number of reporters found in this list probably reflects the conservative nature of our estimates. We studied the *hif-1*-independent, *vgl-1*-dependent gene set using enrichment analysis but no terms were significantly enriched.

## HIF-1 in the cellular context

We identified the transcriptional changes associated with bioenergetic pathways in *C. elegans* by extracting from WormBase all genes associated with the tricarboxylic acid (TCA) cycle, the electron transport chain (ETC) and with the *C. elegans* GO term energy reserve. Previous research has described the effects of mitochondrial dysfunction in eliciting the hypoxia response<sup>11</sup>, but transcriptional control of bioenergetic pathways by HIF-1 has not been studied as extensively in *C. elegans* as in vertebrates (see, for example<sup>12,13</sup>). We also searched for the changes in ribosomal components and the proteasome, as well as for terms relating to immune response (see Fig S5).

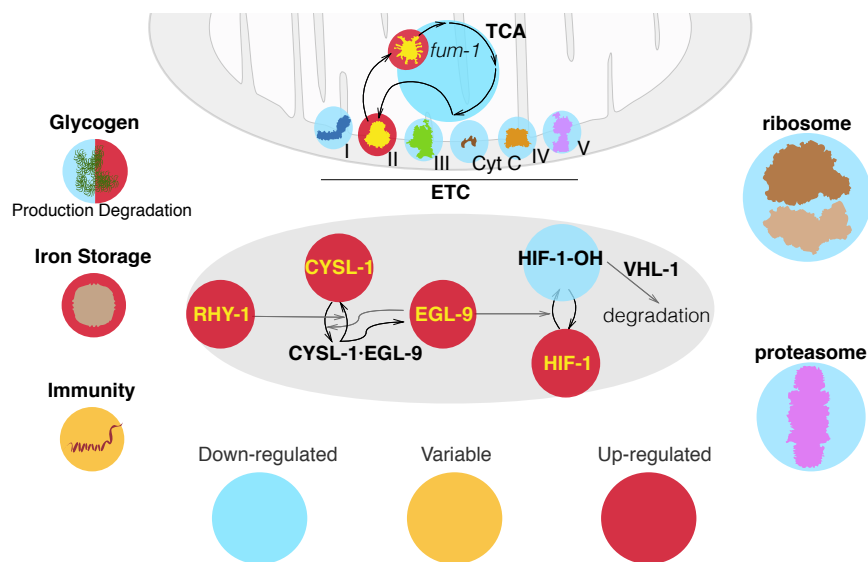


**Figure S5.** A graphic summary of the genome-wide effects of HIF-1 from our RNA-seq data.

## Bioenergetic pathways

Our data shows that most of the enzymes involved in the TCA cycle and in the ETC are down-regulated when HIF-1 is induced in agreement with the previous literature<sup>13</sup>. However, the fumarase gene *fum-1* and the mitochondrial complex II stood out as notable exceptions to the trend, as they were up-regulated in every single genotype that causes deployment of the hypoxia response. FUM-1 catalyzes the reaction of fumarate into malate, and complex II catalyzes the reaction of succinate into fumarate. Complex II has been identified as a source of reserve respiratory capacity in neonatal rat cardiomyocytes previously<sup>14</sup>. We found two energy reserve genes that were down-regulated by HIF-1. *aagr-1* and *aagr-2*, which are predicted to function in glycogen catabolism<sup>15</sup>. Three distinct genes involved in energy reserve were up-regulated. These genes were *oqt-1*, which encodes O-linked GlcNAc Transferase gene; *T04A8.7*, encoding an ortholog

of human glucosidase, acid beta (GBA); and *T22F3.3*, encoding ortholog of human glycogen phosphorylase isozyme in the muscle (PYGM).

## Protein synthesis and degradation

*hif-1(lf)* is also known to inhibit protein synthesis and translation in varied ways.<sup>16</sup> Most reported effects of HIF-1 on the translation machinery are posttranslational, and no reports to date show transcriptional control of the ribosomal machinery in *C. elegans* by HIF-1. We used the WormBase Enrichment Suite Gene Ontology dictionary<sup>?</sup> to extract 143 protein-coding genes annotated as ‘structural constituents of the ribosome’ and we queried whether they were differentially expressed in our mutants. *egl-9(lf)*, *vhl-1(lf)*, *rhy-1(lf)* and *egl-9(lf);vhl-1(lf)* showed differential expression of 91 distinct ribosomal constituents (not all constituents were detected in all genotypes). For every one of these genotypes, these genes were always down-regulated. In contrast, *hif-1(lf)* showed up-regulation of a single ribosomal constituent.

Next, we asked whether HIF-1 has any transcriptional effects on the proteasomal constituents; no such effects of HIF-1 on the proteasome have been reported in *C. elegans*. Out of 40 WormBase-annotated proteasomal constituents, we found 31 constituents whose genes were downregulated in at least two out of the four genotypes we studied. Every gene we found was down-regulated in at least two out of the four genotypes we studied.

## A cellular view of hypoxia

In addition to reconstructing the pathway, our dataset allowed us to observe a wide variety of physiologic changes that occur as a result of the HIF-1-dependent hypoxia response. In particular, we observed down-regulation of most components of the TCA cycle and the mitochondrial electron transport chain with the exceptions of *fum-1* and the mitochondrial complex II. The mitochondrial complex II catalyzes the reaction of succinate into fumarate. In mouse embryonic fibroblasts, fumarate has been shown to antagonize HIF-1 prolyl hydroxylase domain (PHD) enzymes, which are orthologs of EGL-9<sup>17</sup>. If the inhibitory role of fumarate on PHD enzymes is conserved in *C. elegans*, upregulation of complex II by HIF-1 during hypoxia may increase intracellular levels of fumarate, which in turn could lead to elevated levels of HIF-1 even after normoxia resumes. The increase in fumarate produced by the complex could be compensated by increasing expression of *fum-1*. Increased fumarate degradation allows *C. elegans* to maintain plasticity in the hypoxia pathway, keeping the pathway sensitive to oxygen levels.

## References

1. Shao, Z., Zhang, Y. & Powell-Coffman, J. A. Two Distinct Roles for EGL-9 in the Regulation of HIF-1-mediated gene expression in *Caenorhabditis elegans*. *Genetics* **183**, 821–829 (2009).
2. Shen, C., Shao, Z. & Powell-Coffman, J. A. The *Caenorhabditis elegans rhy-1* Gene Inhibits HIF-1 Hypoxia-Inducible Factor Activity in a Negative Feedback Loop That Does Not Include *vhl-1*. *Genetics* **174**, 1205–1214 (2006).
3. Shen, C., Nettleton, D., Jiang, M., Kim, S. K. & Powell-Coffman, J. A. Roles of the HIF-1 hypoxia-inducible factor during hypoxia response in *Caenorhabditis elegans*. *Journal of Biological Chemistry* **280**, 20580–20588 (2005).
4. Park, E. C. *et al.* Hypoxia regulates glutamate receptor trafficking through an HIF-independent mechanism. *The EMBO Journal* **31**, 1618–1619 (2012).
5. Powell-Coffman, J. A. Hypoxia signaling and resistance in *C. elegans*. *Trends in Endocrinology and Metabolism* **21**, 435–440 (2010). URL <http://dx.doi.org/10.1016/j.tem.2010.02.006>.
6. Angeles-Albores, D., N. Lee, R. Y., Chan, J. & Sternberg, P. W. Tissue enrichment analysis for *C. elegans* genomics. *BMC Bioinformatics* **17**, 366 (2016). URL <http://bmcbioinformatics.biomedcentral.com/articles/10.1186/s12859-016-1229-9>.

- 
7. Luhachack, L. G. *et al.* EGL-9 Controls *C. elegans* Host Defense Specificity through Prolyl Hydroxylation-Dependent and -Independent HIF-1 Pathways. *PLoS Pathogens* **8**, 48 (2012). 125 126
  8. Ackerman, D. & Gems, D. Insulin/IGF-1 and hypoxia signaling act in concert to regulate iron homeostasis in *Caenorhabditis elegans*. *PLoS Genetics* **8** (2012). 127 128
  9. Romney, S. J., Newman, B. S., Thacker, C. & Leibold, E. A. HIF-1 regulates iron homeostasis in *Caenorhabditis elegans* by activation and inhibition of genes involved in iron uptake and storage. *PLoS Genetics* **7** (2011). 129 130 131
  10. Semenza, G. L. Hypoxia-inducible factor 1: Regulator of mitochondrial metabolism and mediator of ischemic preconditioning. *Biochimica et Biophysica Acta - Molecular Cell Research* **1813**, 1263–1268 (2011). URL <http://dx.doi.org/10.1016/j.bbamcr.2010.08.006>. 132 133 134
  11. Lee, S. J., Hwang, A. B. & Kenyon, C. Inhibition of respiration extends *C. elegans* life span via reactive oxygen species that increase HIF-1 activity. *Current Biology* **20**, 2131–2136 (2010). URL <http://dx.doi.org/10.1016/j.cub.2010.10.057>. NIHMS150003. 135 136 137
  12. Semenza, G. L., Roth, P. H., Fang, H. M. & Wang, G. L. Transcriptional regulation of genes encoding glycolytic enzymes by hypoxia-inducible factor 1. *The Journal of biological chemistry* **269**, 23757–63 (1994). URL <http://www.ncbi.nlm.nih.gov/pubmed/8089148>. 138 139 140
  13. Semenza, G. L. Hypoxia-inducible factors in physiology and medicine. *Cell* **148**, 399–408 (2012). URL <http://dx.doi.org/10.1016/j.cell.2012.01.021>. 141 142
  14. Pfleger, J., He, M. & Abdellatif, M. Mitochondrial complex II is a source of the reserve respiratory capacity that is regulated by metabolic sensors and promotes cell survival. *Cell Death and Disease* **6**, 1–14 (2015). URL <http://www.nature.com/doifinder/10.1038/cddis.2015.202>. 143 144 145
  15. Sikora, J. *et al.* Bioinformatic and biochemical studies point to AAGR-1 as the ortholog of human acid ??-glucosidase in *Caenorhabditis elegans*. *Molecular and Cellular Biochemistry* **341**, 51–63 (2010). URL <http://link.springer.com/10.1007/s11010-010-0436-3>. 146 147 148
  16. Brugarolas, J. *et al.* Regulation of mTOR function in response to hypoxia by REDD1 and the TSC1 / TSC2 tumor suppressor complex. *Genes and Development* **18**, 1–12 (2004). URL <http://www.pubmedcentral.nih.gov/articlerender.fcgi?artid=534650{&}tool=pmcentrez{&}rendertype=abstract>. 149 150 151 152
  17. Sudarshan, S. *et al.* Fumarate hydratase deficiency in renal cancer induces glycolytic addiction and hypoxia-inducible transcription factor 1alpha stabilization by glucose-dependent generation of reactive oxygen species. *Mol Cell Biol* **29**, 4080–4090 (2009). URL <http://mcb.asm.org/cgi/doi/10.1128/MCB.00483-09{&}5Cnhttp://www.ncbi.nlm.nih.gov/pubmed/19470762>. 153 154 155 156
-